Available online at www.sciencedirect.com
ScienceDirect
Trans. Nonferrous Met. Soc. China 25(2015) 3611−3617
Transactions of Nonferrous Metals Society of China
www.tnmsc.cn

Influence of temperature and strain rate on serration type transition in NZ31 Mg alloy

Wen-hui WANG[1,2], Di WU[2], Rong-shi CHEN[2], Chang-sheng LOU[1]

1. School of Materials Science and Engineering, Shenyang Ligong University, Shenyang 110159, China;
2. Institute of Metal Research, Chinese Academy of Sciences, Shenyang 110016, China

Received 10 January 2015; accepted 2 June 2015

Abstract: The process of tensile test at different temperatures and strain rates was used to study the characteristics of serrated flow, i.e., Portevin-Le Chatelier effect (PLC), in NZ31 Mg alloy. The PLC effect in the tensile stress−strain curves was observed at the temperature range of 150−250 °C. Serrated flow during the deformation at 250 °C is prominent, and a lot of slip bands with a specific direction in each grain can be observed in the microstructure. The serration changes from type A to type C with the increase of temperature and the decrease of strain rate. One single serration of type A was described specifically by the processes of partial pinning, absolute pinning and unpinning. The enhancement of pinning ability at high temperature and low strain rate can promote the absolute pinning process and restrain the unpinning process, which explains the serration type transition.
Key words: NZ31 Mg alloy; Portevin-Le Chatelier effect; serrated flow; serration type

1 Introduction

Mg alloys containing rare-earth elements have been widely used in aerospace and aircraft applications due to their high specific strength and excellent mechanical properties at elevated temperatures [1,2]. As a heat resistant rare earth magnesium alloy Mg−3Nd−1Zn (mass fraction, %), denoted as NZ31, it shows high strength and low cost [3−5]. It has been known that Nd, one of the light rare earth elements, has a maximal solubility (normally 3.6%, mass fraction) in solid Mg at eutectic temperature of 545 °C. Mg−Nd binary alloys have significant strengthening effect [6]. Moreover, the small addition of Zn into Mg−3%Nd alloy would further increase its peak-aged hardness [7,8]. Therefore, this alloy as astronautic structure material has been applied successfully [3].

It was found that serrated flow, i.e., the Portevin-Le Chatelier (PLC) effect, occurred in this alloy during plastic deformation at a certain temperature and strain rate [9]. PLC effect has been commonly accepted as a consequence of dynamic strain aging (DSA), i.e., dynamic pinning and unpinning interactions between the mobile dislocations and solute atoms during plastic deformation, which was first proposed in Al alloys [10−12]. In recent past, serrated flow has also been reported in many Mg alloys, such as Mg−Al−Zn alloy [13], Mg−Y−Nd alloy [14], Mg−Gd alloy [15], Mg−Li alloy [16]. In these reports, many different serration types were found at different deformation temperatures and strain rates. According to the characteristic features, the classification of PLC effect was given by PINK [17] and BRINDLEY and WORTHINGTON [18]. Type A refers to serrations that the general stress raises at first then drops to the original level in curve, otherwise the stress−strain curve is smooth. Type B refers to continuous serrations that the serrate stress raises at first, and then drops to the original level. Type C refers to serrations that only drop below the position in general curve. FANG et al [19] reported that the serration type of PLC effect changed from type A to type A+B and then to type B+C with increasing the temperature from 150 to 300 °C in two Mg−Gd alloys. However, few reports in Mg alloys gave a sound and detailed explanation on the transition of serration type with changing the testing temperature and strain rate.

In this work, the NZ31 alloy after solution treatment,

Foundation item: Project (2013CB632202) supported by the National Basic Research Program of China; Project (51301173) supported by the National Natural Science Foundation of China
Corresponding author: Di WU; Tel: +86-24-23915891; Fax: +86-24-23894149; E-mail: dwu@imr.ac.cn
DOI: 10.1016/S1003-6326(15)64002-X

which ensures a lot of solute atoms in the matrix, was tensile tested at elevated temperatures at different ranges of strain rate and the serrated flow was found under a certain condition. The corresponding mechanism of the serrated flow with different types was discussed on the base of DSA theory, which explained well the serration type transition with the increase of test temperature and strain rate.

2 Experimental

The chemical composition of NZ31 alloy was Mg−2.7Nd−0.6Zn−0.5Zr (mass fraction, %). It was prepared with Mg (purity 99.95%), Zn (99.9%), Nd (99.5%) and Mg−30Zr by melting them in an electric resistance furnace under the protection of RJ-6 anti-oxidizing flux, which was mainly composed of 54%−56% KCl, 27%−29% $CaCl_2$, 14%−16% $BaCl_2$ and 1.5%−2.5% NaCl (mass fraction) [20]. The ingots with dimensions of 75 mm × 200 mm × 200 mm were prepared by pouring the melted alloy into a preheated steel mold. They were homogenized at 525 °C for14 h, and then quenched in water.

The sheets for tensile tests were cut from the casting ingots with a gauge length of 10 mm, width of 4 mm and thickness of 2.5 mm. They were tested using a Sans type tensile testing machine equipped with a heating chamber. Tensile tests were conducted at temperature from 100 to 300 °C with a strain rate of 1×10^{-3} s^{-1}. At the temperature of 250 °C, tensile tests were conducted with the strain rates ranging from 1×10^{-4} to 1×10^{-2} s^{-1}. A tensile test with repeatedly varying strain rates of 1×10^{-4} and 1×10^{-3} s^{-1} at 250 °C was completed. During the tensile test, the specimens were kept at a given temperature with the deviation less than 2 °C. The samples were held for about 10 min prior to the test to eliminate the temperature gradient. To ensure the accuracy of results, the final data of tensile tests were based on the average results of three specimens.

For microstructure observation, the samples were cut from the gauge part of the tensile test bars with the observation plane perpendicular to the thickness direction and then etched by a solution of HNO_3 (5%, volume fraction) in ethanol after mechanical polishing to observe the grain boundaries. The microstructures were examined using an optical microscope (OM), a confocal laser scan microscope (LEXT, Olympus OLS4100), a scanning electron microscope (SEM, Philips XL30 ESEM−FEG/EDAX) equipped with an energy-dispersive X-ray (EDX) spectroscopy analysis system, and a transmission electron microscope (TEM, JEM−2100F) operating at 200 kV. The thin foil specimens for TEM observation were prepared by punching discs of 3 mm in diameter, followed by dimple grinding and Ar^+ ion milling in a precision ion polishing system (PIPS, Gatan) operating at accelerating voltage of 4.5 kV and incident angle of ~8°.

3 Results

The typical engineering stress−strain curves at a temperature range of 100−300 °C are shown in Fig. 1(a). The results show that the serrated flow (PLC effect) is present only within the temperature range of 150−250 °C, and the curves are smooth at 100 and 300 °C. As shown in Fig. 1(b), type A serration dominates at 150°C, and the period and amplitude of serrations are longest and lowest, respectively, in comparison with those of serrations at other temperatures. At 200 °C, the serration type changes to A+B that exhibits an increase of the frequency of serrations. As the temperature increases to 250 °C, the serrations evolve into type B, where the frequency and amplitude of serrations become the most intense.

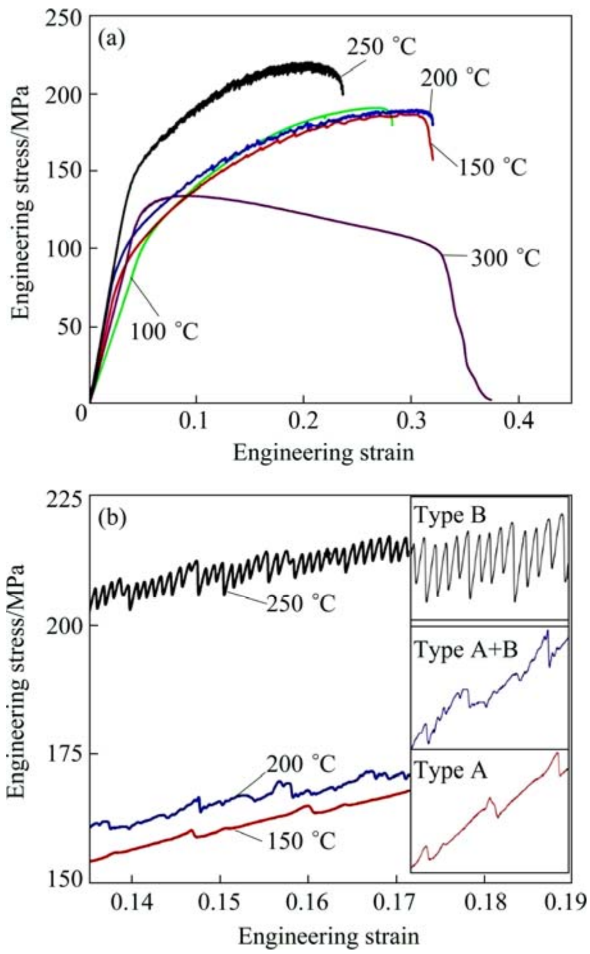

Fig. 1 Engineering stress−strain curves (a) and types of serration (b) at temperature range of 100−250 °C with strain rate of 1×10^{-3} s^{-1} for NZ31 alloy

The typical engineering stress−strain curves at 250 °C with the strain rate ranging from 1×10^{-4} to

1×10^{-2} s^{-1} are shown in Fig. 2. Among the strain rate range of 1×10^{-4}−1×10^{-3} s^{-1}, the frequency of serrations increases with the increase of strain rate, and the type of serrated flow starts with type C and then evolves into type B.

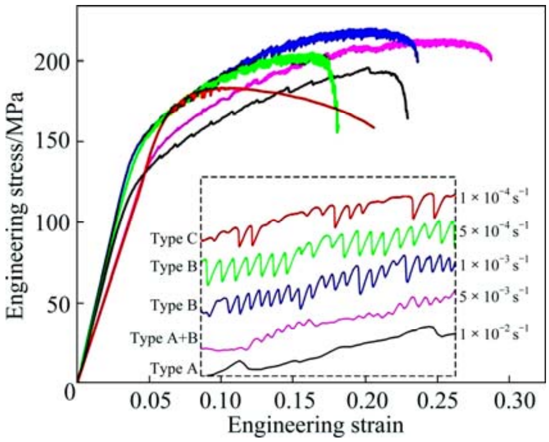

Fig. 2 Engineering stress−strain curves obtained at different strain rates and temperature of 250 °C for NZ31 alloy

Among the strain rate range of 1×10^{-3}−1×10^{-2} s^{-1}, the frequency of serrations decreases with the increase of strain rate, and the serrated flow starts with type B and then evolves into type A. The amplitude of serrations at low strain rate is bigger than that at high strain rate.

The critical strain of PLC effect, i.e., the onset of serrated flow, is shown in Fig. 3. As shown in Fig. 3(a), at the strain rate of 1×10^{-3} s^{-1}, the critical strain decreases with the increase of temperature. As shown in Fig. 3(b), at the temperature of 250 °C, the critical strain decreases firstly and then increases with increasing the strain rate from 1×10^{-4} to 5×10^{-2} s^{-1}. At the strain rate of 5×10^{-3} s^{-1}, the value of critical strain reaches the minimum.

The relationship of the yield strength (YS), ultimate tensile strength (UTS) and elongation-to-fracture (EL) with temperature at strain rate of 1×10^{-3} s^{-1} of NZ31 Mg alloy are shown in Fig. 4. With increasing the temperature from 100 to 200 °C, the UTS varies a little and the YS decreases gradually, while the EL increases with a narrow range. As the test temperature increases to 250 °C, the UTS and YS increase markedly and reach the maximum value points, which expresses an abnormal mechanical behavior. In addition, the EL decreases to the minimum value. With the temperature increasing from 250 to 300 °C, the UTS decreases distinctly, whereas the EL increases by a large margin.

Figure 5 presents the microstructures of NZ31 alloy under solutionized condition before and after tensile test at 250 °C. As can be seen from Fig. 5(a), the original OM image, a few of residual eutectic compounds form in triple junctions at grain boundaries. When the tensile test

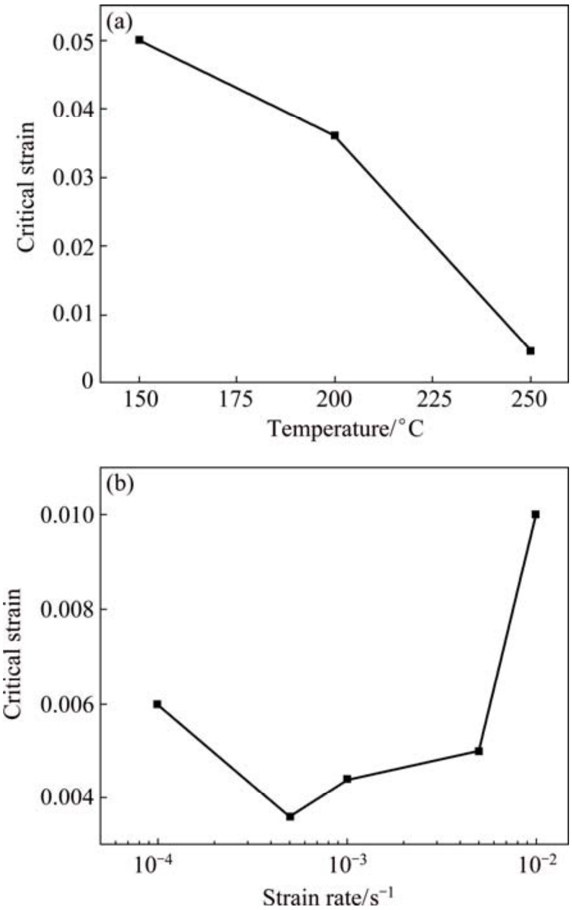

Fig. 3 Critical strain of PLC effect at temperature range of 100−250 °C with strain rate of 1×10^{-3} s^{-1} (a) and at temperature of 250 °C with different strain rates (b) for NZ31 alloy

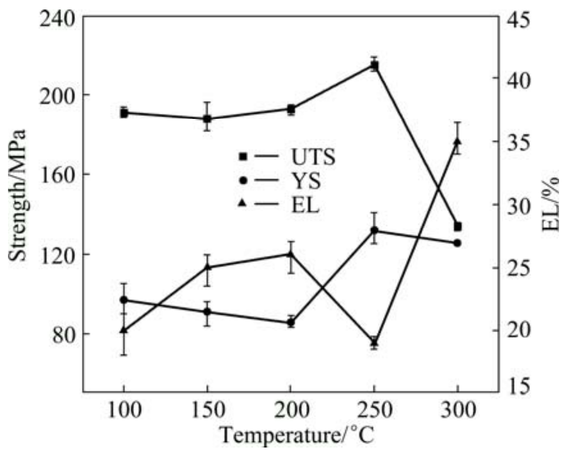

Fig. 4 Temperature dependence of yield strength, ultimate tensile strength and elongation-to-fracture of samples

was performed at 250 °C, the serrated flow with type B was significant. So, this test condition was selected for the LEXT, SEM and TEM microstructures observation. As can be seen from Fig. 5(b), a lot of slip bands with a specific direction in each grain can be observed, which means a large amount of dislocation slips happened during the tensile test. Many dislocations gather in the

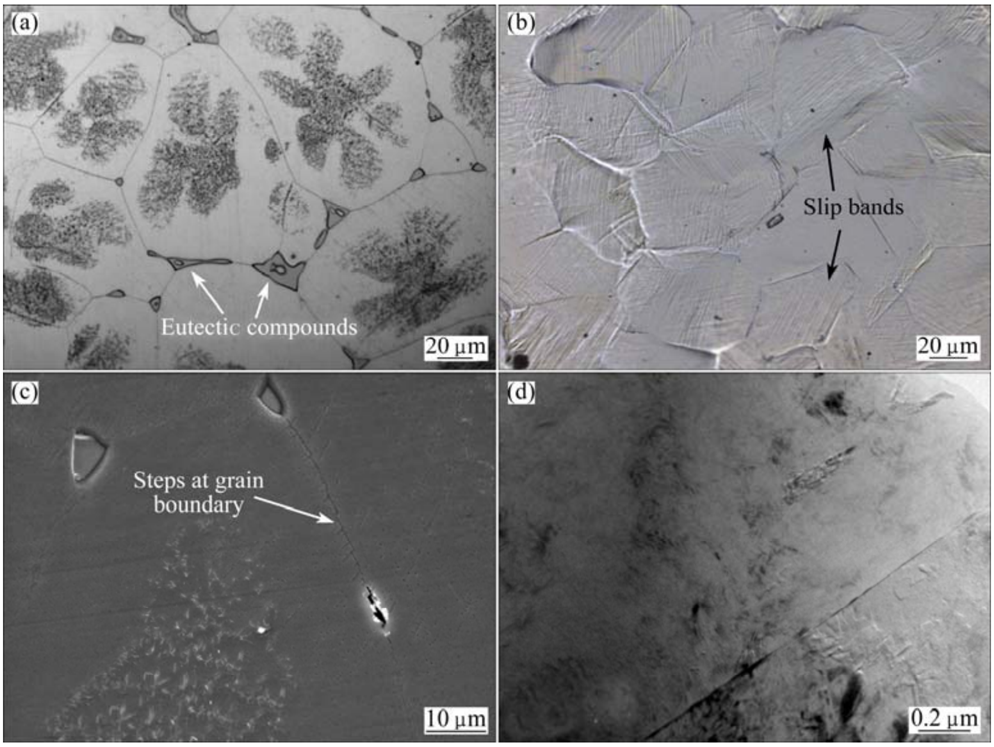

Fig. 5 Optical microstructure of solutionized NZ31 alloy before tensile test (a), LEXT image (b), SEM image (c) and TEM image (d) after tensile test at 250 °C

grain boundaries, causing the steps of grain boundaries, as shown in Fig. 5(c). As can be seen from Fig. 5(d), the TEM image shows few precipitates produced in the grain matrix after the tensile test at 250 °C. Therefore, the serrated flow in NZ31 alloy should be attributed to the interaction between the solute atoms and dislocations, i.e., the DSA theory, rather than the shearing precipitates by dislocations [21].

4 Discussion

4.1 Detailed description of type A serration

One type A serration which happened at 150 °C was observed and is shown in Fig. 6. It is worth noting that the type A serration consists of three distinct processes: at first, the stress increases slowly, then increases rapidly, and finally suddenly drops. Based on the DSA theory, the mechanism of the three processes of serration A is detailedly described in Fig. 7. At the beginning of serrated flow, when the mobile dislocations are hindered temporarily by the obstacles such as forests and precipitates [11], the solute atoms start to gather in the dislocations by diffusion [21,22]. Therefore, these solute atoms cause the mobile dislocations decelerate as well as provide an additional dragging stress in system [12]. As the moving rate of dislocation turns to slow, it becomes easier for more solute atoms to diffuse into the dislocation. In this process, more and more solute atoms

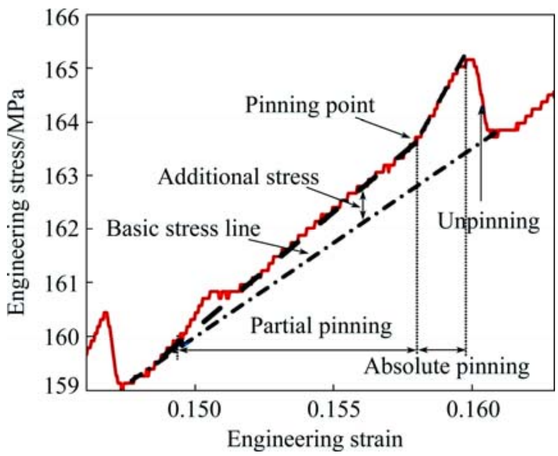

Fig. 6 Detailed description of one serration of type A at 150 °C

gather in the dislocation and drag it (Fig. 7(c)), resulting in the moving rate of dislocation continuously decreasing and the additional stress continuously increasing, as shown in Fig. 6. Therefore, the process that the stress increases slowly is defined as partial pinning. It is worth noting that in this process, both the strain hardening effect and partial pinning effect make a contribution to the increase of stress with increasing the strain. The strain hardening comes from the interaction between dislocations [23], while the partial pinning process is caused by the interaction between the dislocation and solute atoms. As shown in Fig. 6, the basic stress line which connects the two adjacent points just after unpinning may qualitatively represent the increase of stress without DSA effect between solute atoms and dislocation, but which contains the interaction between dislocations. In a series of contiguous serrations, this contiguous basic stress line approximately presents a usual stress−strain curve with strain hardening (Fig. 8). Accordingly, on the whole, the upward additional stress above the basic stress line is manly caused by the pinning effect of solute atoms, and the contribution of strain hardening in stress roughly increases along the basic stress line with the increase of strain.

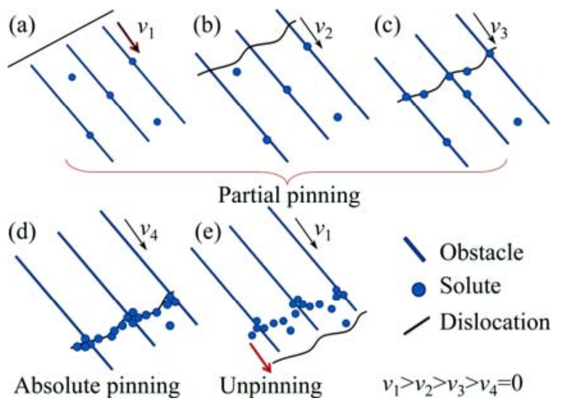

Fig. 7 Sketch map of mechanism of partial pinning (a−c), absolute pinning (d) and unpinning (e) in type A serration

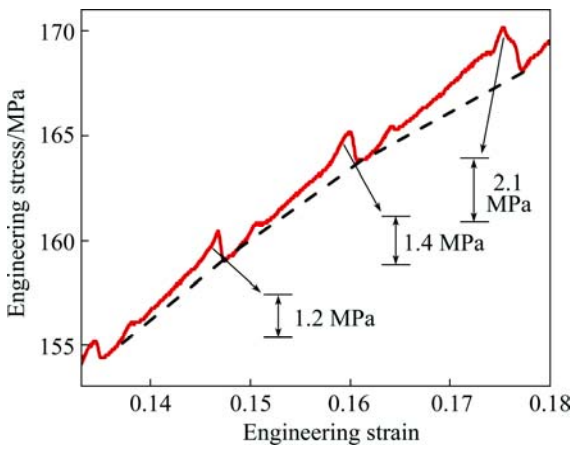

Fig. 8 Amplitude of type A serrated flow at 150 °C

At the pinning point, the number of the solute atoms gathering in the dislocation is much enough to absolutely pin the dislocation and make it motionless (Fig. 7(d)). As the strain continues to increase, there must present a strong elastic interaction between the pinned dislocation and the gathering solute atoms, leading to a rapid increase of stress after the pinning point (Fig. 6). So this process is termed as absolute pinning process.

As the process of absolute pinning developing, the aid of applied stress causes the dislocations to move again (Fig. 7(e)), and then the pinned dislocations get escape from the solute atoms by thermal activation process called unpinning [24]. As a result, the stress also decreases rapidly as the mobile dislocations get free from the solute atoms (Fig. 6).

The number of dislocations, i.e., dislocation density, increases with the increase of strain. So, more dislocations are absolutely pinned, higher stress need to be applied for unpinning. Therefore, the amplitude, i.e., the stress drop during unpinning process of type A serration, increases with the increase of strain, as shown in Fig. 8.

4.2 Type transition of serration with temperature and strain rate

In samples deformed with a constant temperature and strain rate, three different types of serration can be observed, usually referred to as types A, B and C, and the serration type transits from type A to C with the increase of temperature or the decrease of strain rate [25]. The serration type transition can be associated with the number of dislocations participating in the band or the diffusion process of solute atoms [26], and the plastic deformation band discontinuous transmission in space [27].

The current work discusses the process of partial pinning, absolute pinning and unpinning with different temperatures and strain rates. The change of three processes results in the serration type transition. In NZ31 Mg alloy, the serration changes from type A into type A+B, and finally into type B with the increase of temperature at the strain rate of 1×10^{-3} s^{-1}. Type A serration at 150 °C includes three processes of partial pinning, absolute pinning and unpinning processes. With increasing the temperature up to 200 °C, the diffusion rate of solutes increases [28]. Therefore, the time during which solute atoms gather in dislocations until forming an absolute pinning turns short, thus the process of partial pinning decreases. Thus, the serration starts with type A and then evolves into type A+B. As the temperature increases to 250 °C, the diffusion rate of solute atoms turns so high that the partial pinning nearly disappears and starts with absolute pinning. As a consequence, the serration evolves into type B, making up of two processes which are absolute pinning and unpinning processes.

The serration changes from type A into type B, finally into type C with the decrease of strain rate at 250 °C. At high strain rate, such as 1×10^{-2} s^{-1}, in comparison with the diffusion ability, the strain rate is a dominating factor. The moving rate of dislocations is so fast that the diffusion of solute atoms to dislocations turns more difficult in comparison with that at the strain rate of 1×10^{-3} s^{-1}. Therefore, the time during which solute atoms gather in dislocations until absolute pinning turns long, thus the process of partial pinning increases. As a result, the type A serration forms.

At low strain rate such as 1×10^{-4} s^{-1}, the diffusion ability is a dominating factor in comparison with that at the strain rate of 1×10^{-3} s^{-1}. The moving rate of dislocation becomes so slow that the diffusion of solute atoms to dislocations turns more easy. The solute atoms can pin the dislocations instantaneously at the strain rate of 1×10^{-4} s^{-1}, and the solute atoms are possible to move with dislocations at the low strain rate. As a result, the dislocations start with pinning before critical strain and then start with unpinning process [24]. Therefore, the serrated flow consists of unpinning and absolute pinning, and the type C serration starts to form.

At a medium strain rate of 1×10^{-3} s^{-1}, both the diffusion ability and strain rate dominate the serrated flow. The high diffusion rate of solute atoms causes absolute pinning forming fast, and the dislocations also move so rapidly that the unpinning process can be brought into easily after absolute pinning. Therefore, the serrations begin with the process of absolute pinning and then end at unpinning process which is the type B serration.

The result of tensile test with varying strain rate is shown in Fig. 9, which is highly consistent with the mechanism described above. At low strain rate of 1×10^{-4} s^{-1}, more solute atoms gather in the dislocations, simultaneously form absolute pinning and drag the dislocation to move with it. So, it exhibits a higher flow stress than that at high strain rate of 1×10^{-3} s^{-1}, i.e., negative strain rate sensitivity.

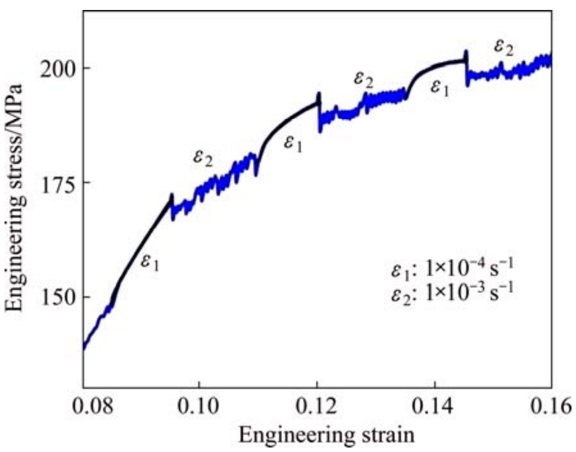

Fig. 9 Variation strain rate dependence of engineering stress−strain curve at 250 °C

5 Conclusions

1) The PLC effect and tensile property in NZ31 Mg alloy were studied at different temperatures and strain rates.

2) One single serration of type A was described specifically by the processes of partial pinning, absolute pinning and unpinning.

3) Based on the DSA theory, the mechanism of the three processes of serration A was established, which is consistent with the experimental results, and well explains the serration type transition with temperature and strain rate.

References

[1] WU Di, TANG Wei-neng, CHEN Rong-shi, HAN En-hou. Strength enhancement of Mg−3Gd−1Zn alloy by cold rolling [J]. Transactions of Nonferrous Metals Society of China, 2013, 23(2): 301−306.

[2] NIE J F, MUDDLE B C. Characterisation of strengthening precipitate phases in a Mg–Y–Nd alloy [J]. Acta Materialia, 2000, 48(8): 1691−1703.

[3] NING Z L, WANG G J, CAO F Y, SUN J F, DU J F. Tensile deformation of a Mg−2.54Nd−0.26Zn−0.32Zr alloy at elevated temperature [J]. Journal of Materials Science, 2009, 44(16): 4264−4269.

[4] WANG Shao-hua, GUO Xing-wu, SUN Can, GONG Jia, PENG Li-ming, DING Wen-jiang. Electrodeposition of Cu coating with high corrosion resistance on Mg−3.0Nd−0.2Zn−0.4Zr magnesium alloy [J]. Transactions of Nonferrous Metals Society of China, 2014, 24(12): 3810−3817.

[5] MA L, MISHRA R K, BALOGH M P, PENG L, LUO A A, SACHDEV A K, DING W. Effect of Zn on the microstructure evolution of extruded Mg–3Nd(–Zn)–Zr (wt.%) alloys [J]. Materials Science and Engineering A, 2012, 543: 12−21.

[6] HONMA T, OHKUBO T, HONO K, KAMADO S. Chemistry of nanoscale precipitates in Mg−2.1Gd−0.6Y−0.2Zr (at.%) alloy investigated by the atom probe technique [J]. Materials Science and Engineering A, 2005, 395(1−2): 301−306.

[7] LI Q, WANG Q, WANG Y, ZENG X, DING W. Effect of Nd and Y addition on microstructure and mechanical properties of as-cast Mg−Zn−Zr alloy [J]. Journal of Alloys and Compounds, 2007, 427(1−2): 115−123.

[8] SANATY-ZADEH A, XIA X, LUO A A, STONE D S. Precipitation evolution and kinetics in a magnesium−neodymium−zinc alloy [J]. Journal of Alloys and Compounds, 2014, 583: 434−440.

[9] WU D, CHEN R S, KE W. Microstructure and mechanical properties of a sand-cast Mg−Nd−Zn alloy [J]. Materials and Design, 2014, 58: 324−331.

[10] COTTRELL A H. A note on the Portevin-Le Chatelier effect [J]. Philos Mag, 1953, 44: 829−832.

[11] McCORMICK P G. A model for the Portevin-Le Chatelier effect in substitutional [J]. Acta Metallurgica, 1972, 20(3): 351−354.

[12] PENG K, CHEN W, QIAN K. Study on dynamic strain aging phenomenon of 3004 aluminum alloy [J]. Materials Science and Engineering A, 2006, 415(1−2): 53−58.

[13] CORBY C, CACERES C H, LUKA P. Serrated flow in magnesium alloy AZ91 [J]. Materials Science and Engineering A, 2004, 387: 22−24.

[14] ZHU S M, NIE J F. Serrated flow and tensile properties of a Mg−Y−Nd alloy [J]. Scripta Materialia, 2004, 50(1): 51−55.

[15] WU D, CHEN R S, HAN E H. Serrated flow and tensile properties of a Mg−Gd−Zn alloy [J]. Materials Science and Engineering A, 2012, 532: 267−274.

[16] WANG C. Serrated flow and abnormal strain rate sensitivity of a magnesium−lithium alloy [J]. Materials Letters, 2006, 60(24): 2941−2944.

[17] PINK E. The effect of precipitates on characteristics of serrated flow

in AlZn5Mg1 [J]. Acta Metallurgica, 1989, 37(7): 1773−1781.

[18] BRINDLEY B J, WORTHINGTON P J. Serrated yielding in aluminium−3% magnesium [J]. Acta Metallurgica, 1969, 17(11): 1357−1361.

[19] FANG X Y, YI D Q, NIE J F. The serrated flow behavior of Mg−Gd(−Mn−Sc) alloys [J]. Metallurgica and Materals Transactions A, 2009, 40(11): 2761−2770.

[20] Q J. Smelting standard of cast magnesium alloy [S]. 1989.

[21] SLEESWYK A W. Slow strain-hardening of ingot iron [J]. Acta Metallurgica, 1958, 6(9): 598−603.

[22] NORTMANN A, SCHWINK C. Characteristics of dynamic strain ageing in binary FCC copper alloys [J]. Acta Metallurgica, 1997, 45(5): 2043−2051.

[23] KOCKS U F, MECKING H. Physics and phenomenology of strain hardening: The FCC case [J]. Progress in Materials Science, 2003, 48(3): 171−273.

[24] FU S H, CHENG T. ZHANG Q C. Two mechanisms for the normal and inverse behaviors of the critical strain for the Portevin-Le Chatelier effect [J]. Acta Materialia, 2012, 60(19): 6650−6656.

[25] KUBIN L P, FRESSENGEAS C, ANANTHAKRISHNA G. Dislocations in solids [M]. North Holland: Elsevier, 2002.

[26] SARKAR A, CHATTERJEE A, BARAT P, MUKHERJEE P. Comparative study of the Portevin-Le Chatelier effect in interstitial and substitutional alloy [J]. Materials Science and Engineering A, 2007, 459(1−2): 361−365.

[27] BRART P, SARKAR A, MUKHERJEE P, BANDYOPADHYAY S K. Scaling behavior of the Portevin-Le Chatelier effect in an Al−2.5Mg alloy [J]. Physical Review Letters, 2005, 94(5): 255502.

[28] van DEN BEUKEL A. On the mechanism of serrated yielding and dynamic strain ageing [J]. Acta Metallurgica, 1980, 28(7): 965−969.

温度及应变速率对 NZ31 镁合金锯齿流变类型转变的影响

王文辉 [1,2]，吴 迪 [2]，陈荣石 [2]，娄长胜 [1]

1. 沈阳理工大学 材料科学与工程学院，沈阳 110159；

2. 中国科学院 金属研究所，沈阳 110016

摘 要：将固溶处理后的 NZ31 镁合金在不同温度及应变速率下进行拉伸实验，研究温度及应变速率对锯齿流变(Portevin-Le Chatelier 效应)特征的影响。合金的锯齿流变行为出现在温度为 150 到 250 °C 之间，在 250 °C 时表现最剧烈，并且在晶粒内部可以发现特定取向的滑移带。随着温度的升高或应变速率的降低，锯齿流变类型由 A 型逐渐转变成 C 型。单个 A 型锯齿可划分为局部钉扎、完全钉扎和脱钉三个阶段。当温度升高或者应变速率降低时，溶质原子钉扎能力的增强会促进完全钉扎阶段的形成或者抑制脱钉阶段的发生，从而引起锯齿类型的转变。

关键词：NZ31 镁合金；Portevin-Le Chatelier 效应；锯齿流变；锯齿类型

(Edited by Mu-lan QIN)